LEBIM PREDICTIONS FOR FIBRE-MATRIX DEBONDS IN UNIDIRECTIONAL FIBRE-REINFORCED COMPOSITES UNDER BIAXIAL TRANSVERSE LOADS

Luis Távara, Vladislav Mantič, Enrique Graciani, Federico París

Grupo de Elasticidad y Resistencia de Materiales, Escuela Técnica Superior de Ingeniería,
Universidad de Sevilla, Camino de los Descubrimientos s/n, 41092 Sevilla, Spain
Email: ltavara@us.es, Web Page: http://www.germus.es

Keywords: Debonding, Fracture toughness, Interfacial strength, Failure criterion, Transverse cracking

Abstract

Fibre–matrix interface debond onset and growth in a bundle of fibres are studied numerically. A fibre bundle subjected to far field biaxial transverse loads is considered. The Linear Elastic–Brittle Interface Model (LEBIM) is used to model the fibre–matrix interface cracks behaviour. The model of an actual unidirectional lamina includes ten fibres embedded in a matrix cell whose external dimensions were much larger than the fibre radius. Similar results were previously obtained for the single fibre model by the authors. The novelty of the present model based on the LEBIM formulation lies in its ability to make quantitative predictions about the concurrent fibre–matrix debond onset and mixed–mode interface crack growth in a fibre bundle. The prediction of the failure loads (critical loads) producing the first debond onset in a small fibre bundle is one the aims of the present work. Results also verify the unstable growth of subsequent debonds under transverse loads. Some aspects of the failure mechanisms of an actual composite material under transverse loads are elucidated by studying the effect of the load biaxility in this simplified problem.

1. Introduction

At the microscale, the level of interaction between fibres and matrix, the role of interfaces and interphases is well recognized, see [1–3] and references therein. It is well known that the interfaces between the constituents of composite materials play a significant role in failure mechanisms [4–7]. Experimental, numerical and semi-analytical studies of the inter-fibre failure (also called matrix failure) of a single fibre embedded in a matrix under biaxial transverse loads developed by the present authors and coworkers can be found in [3, 8–12]. These works show the influence of a secondary transverse load (tension or compression) applied perpendicularly to the primary transverse tension (thus creating a biaxial state) on the generation of the damage dominated by the primary transverse tension.

The collocational Boundary Element Method (BEM) and Linear Elastic – (perfectly) Brittle Interface Model (LEBIM) are used to study and characterize the behaviour of the fibre-matrix interface in [2, 3, 13]. In these works failure curves in which both tensile and compressive loads are considered are obtained for a single fibre model and a ten-fibre model.

Although, several works have been devoted to study the fibre-matrix interface debond problem, there are still some open issues regarding it. In the present work, the BEM is applied to obtain a numerical solution for a sequence of fibre-matrix interface crack onsets and growths at different fibres in the above

Excerpt from ISBN 978-3-00-053387-7

mentioned problem. The numerical results include a study of the positions where the first debond occurs in the fibre-matrix system, which will have a great influence on the final macro–crack path shape.

2. LEBIM

The continuous spring distribution that models an elastic layer (interphase) along a fibre-matrix interface is governed by the following simple linear elastic-(perfectly) brittle law[1] written at an interface point x:

$$\begin{array}{ll} \text{Linear Elastic} & \left\{ \begin{array}{l} \sigma(x) = k_n \delta_n(x), \\ \tau(x) = k_t \delta_t(x), \end{array} \right. \qquad G(x) < G_c(\psi(x)), \\ \text{interface (undamaged)} & \\ \text{Broken} & \left\{ \begin{array}{l} \sigma(x) = k_n \langle \delta_n(x) \rangle_-, \\ \tau(x) = 0. \end{array} \right. \\ \text{interface} & \end{array} \tag{1}$$

where $\sigma(x)$ and $\tau(x)$ are, respectively, the normal and tangential components of the tractions in the elastic layer along the interface, $\delta_n(x)$ and $\delta_t(x)$ are, respectively, the normal and tangential relative displacements between opposite interface points. k_n and k_t denote the normal and tangential stiffnesses of the spring distribution. It is assumed that the crack tip at x advances (or the interface breaks at point x) when the corresponding Energy Release rate (ERR) $G(x)$ reaches the critical ERR value $G_c(\psi(x))$, that is $G(x) = G_c(\psi(x))$, where $\tan^2 \psi = \frac{G_{II}}{G_I}$ for $G_I > 0$. The extended energetic fracture-mode-mixity angle ψ is defined by, see [3]:

$$\tan \psi = \sqrt{\xi^{-1}} \tan \psi_\sigma = \sqrt{\xi} \tan \psi_u, \tag{2}$$

where $\xi = k_t/k_n$, $\tan \psi_\sigma = \tau/\sigma$ and $\tan \psi_u = \delta_t/\delta_n$, ψ_σ and ψ_u being the stress and relative displacement based fracture-mode-mixity angles, respectively. The ERR of the linear elastic interface at a point x is defined as, cf. [3, 14–17]: $G(x) = G_I(x) + G_{II}(x)$, with

$$G_I(x) = \frac{\sigma(x)\langle \delta_n(x) \rangle_+}{2}, \qquad G_{II}(x) = \frac{\tau(x)\delta_t(x)}{2}, \tag{3}$$

verifying $G_I = 0$ for $\delta_n \leq 0$. The functional dependence of G_c on the fracture-mode-mixity angle ψ is defined similarly as in [18] with a slight modification [3] as follows,

$$G_c = G_{Ic}[1 + \tan^2((1 - \lambda)\psi)], \tag{4}$$

where

$$G_{Ic} = \frac{\bar{\sigma}_c \bar{\delta}_{nc}}{2} = \frac{\bar{\sigma}_c^2}{2k_n} = \frac{k_n \bar{\delta}_{nc}^2}{2} \tag{5}$$

corresponds to the fracture energy in pure opening mode I. λ is a fracture-mode-sensitivity parameter (usually obtained from the best fit of experimental results), $\bar{\sigma}_c > 0$ and $\bar{\delta}_{nc} > 0$ are the critical normal component of traction and normal relative displacement in mode I, i.e. $\bar{\sigma}_c = k_n \bar{\delta}_{nc} = \sigma_c(\psi = 0)$ and $\bar{\delta}_{nc} = \delta_{nc}(\psi = 0)$.

In summary, LEBIM needs the input of four independent variables: $\bar{\sigma}_c$, G_{Ic}, ξ and λ. Typical range $0.2 \leq \lambda \leq 0.3$ characterizes interfaces with moderately strong fracture-mode-dependence [18]. Further details on the deduction of the above criterion are presented in [2, 3, 13].

[1] The positive and negative part of a real number δ are defined in the present work as $\langle \delta \rangle_\pm = \frac{1}{2}(\delta \pm |\delta|)$. $\langle \cdot \rangle_+$ is also referred to as Macaulay brackets or ramp function.

Excerpt from ISBN 978-3-00-053387-7

3. Ten-fibre problem

3.1. Description of the problem

The problem of a bundle of ten circular inclusions with radius a, embedded in an infinite (very large) matrix, is numerically solved. The position of the fibres corresponds to a randomly selected portion of an actual glass fibre composite micrograph [13], see Figure 1. Both the inclusions and matrix are considered as linear elastic isotropic materials. A plane strain state is assumed in this bimaterial system. Let (x, y) be the cartesian coordinates. The uniform remote loads σ_x^∞ and σ_y^∞ are parallel to the x-axis (horizontal) and y-axis (vertical), respectively. Different values of the load biaxiality ratio [3, 13]:

$$\chi = \frac{\sigma_x^\infty + \sigma_y^\infty}{2\ \max\{|\sigma_x^\infty|, |\sigma_y^\infty|\}}, \tag{6}$$

are considered, with $\chi = -0.5$ defining pure compression in one direction, $\chi = 0$ equibiaxial tension-compression (pure shear), $\chi = 0.5$ pure tension in one direction, and $\chi = 1$ equibiaxial tension. Values of χ in the interval $-0.5 \leq \chi \leq 1$ are considered hereinafter.

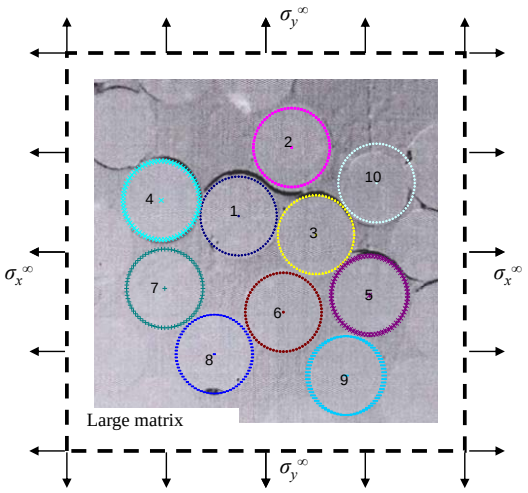

Figure 1. Selected fibres obtained from a glass fibre composite micrograph and far field transverse loads.

Remote loads σ_x^∞ and σ_y^∞ are applied along the sides of a large square matrix that surrounds the fibres located approximately at the centre of the square. In order to see the influence of the random positions of the fibres, the bundle of fibres has been rotated by angles 15°, 30°, 45°, 60° and 75° with respect to the x-axis,

3.2. Model of the problem

A typical bimaterial system among fibre reinforced composite materials is chosen for this study: epoxy matrix (m) and glass fibre (f). The elastic properties of the matrix and fibre are $E_m = 2.79$ GPa, $\nu_m = 0.33$, $E_f = 70.8$ GPa and $\nu_f = 0.22$. The fibre-matrix interface fracture toughness in mode I and critical tension of the interface assumed in the present work are respectively: $G_{Ic} = 2$ Jm^{-2} and $\bar{\sigma}_c = 90$ MPa. A fixed relation between k_n and k_t ($\xi = 0.25$) is chosen. The fracture-mode-sensitivity parameter is defined as $\lambda = 0.25$.

After the initial condition of the undamaged interfaces, a linear analysis is carried out to calculate which

Excerpt from ISBN 978-3-00-053387-7

interface node (spring) reaches first its critical ERR value. This linear analysis will be the first step and the calculated critical load causes the onset of the first debond at some fibre-matrix interface. Then, the solution algorithm makes a sequence of similar linear analyses where the interface points (springs) that had reached the critical value in the previous step switch their interface condition (from undamaged to broken springs). Each linear analysis becomes a new step and its critical load corresponds to the load that causes a new debond growth or onset. This procedure is usually called as Sequential Linear Analysis (SLA) [3].

The 2D BEM model represents ten circular inclusions, see Figure 1, with radius a =7.5 μm inside a relatively large square matrix with a 1 mm side (2ℓ = 1mm). 3632 continuous linear boundary elements are used: 32 elements for the external boundary of the matrix cell and two uniform meshes (for each fibre) of 180 elements to model each fibre-matrix interface (therefore, the polar angle of each element at the interface is 2°).

4. Numerical Results

4.1. Behaviour of the debonds

Figure 2(a), shows the values of the normalized far-field load needed for the first debond onset (first step) and the load needed in each subsequent step to produce either a debond growth or an onset of a new debond. The cases shown are $\chi = 0$ (equibiaxial state of tension in the y-direction and compresion in the x-direction – TC), $\chi = 0.5$ (uniaxial tension in the y-direction – T) and $\chi = 1$ (equibiaxial tension – TT) with no rotation of the bundle of fibres with respect to the coordinate system (red, blue and green lines, respectively). The (first) critical loads σ^{∞}_{cy} (critical load in the y-direction) are indicated by dotted lines.

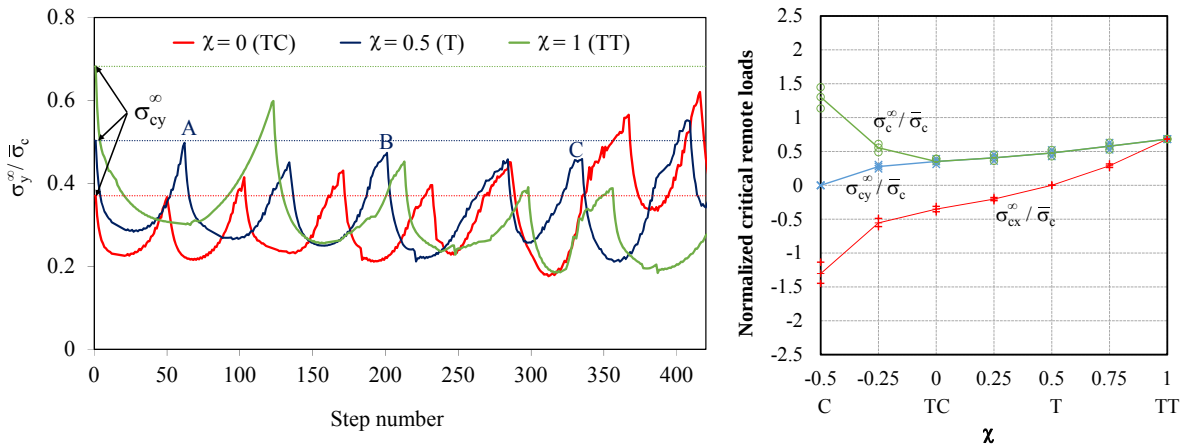

(a) (b)

Figure 2. (a) Far-field load σ^{∞}_{y} (for $\sigma^{\infty}_{y} \geq \sigma^{\infty}_{x}$) needed in each step to produce either a debond onset or debond growth for $\chi = 0, 0.5$ and 1. Each step essentially corresponds to the extension of the total cracked interface length by 2°. (b) Load biaxility effect on the first critical remote loads σ^{∞}_{cx} and σ^{∞}_{cy}.

As shown in Figure 2(a) three different kind of curves may be obtained, roughly speaking. The first one (red, for $\chi = 0$ – TC) shows that after an unstable growth of a debond, a larger load is necessary to produce a subsequent debond. It can be said that the fracture process of subsequent debond onsets from fibre to fibre is "globally stable". In the second kind of curve (blue, for $\chi = 0.5$ – T) a very similar load is necessary to produce a subsequent debond. Thus, the fracture process of subsequent debond onsets from fibre to fibre is "globally in neutral equilibrium". Finally, in the third kind of curve (green, for $\chi = 1$

Excerpt from ISBN 978-3-00-053387-7

– TT) the first critical load, σ_{cy}^{∞} (load necessary to produce the first debond), and the corresponding σ_{cx}^{∞}, produces not only the first fibre debond but it also produces several subsequent fibre debonds, since significantly lower loads are needed to produce these debonds. Thus, the fracture process of subsequent debond onsets from fibre to fibre is "globally unstable" [13].

From all the cases solved numerically for different values of the biaxiality ratio χ and different rotations of the fibre bundle, it is possible to study the biaxility effect on the first critical remote loads (in both directions), see Figure 2(b). The average load is shown as the continuous line, while the scatter obtained (minimum and maximum load values) is represented by the markers [13]. It is also interesting to notice that according to Figure 2(b), the most critical (dangerous) biaxial condition is reached for $\chi = 0$ (TC case), where the minimum values of σ_c^{∞} are obtained (with $\sigma_c^{\infty} = \max\{|\sigma_{cx}^{\infty}|, |\sigma_{cy}^{\infty}|\}$), in accordance to previous experimental results by París et. al. [8]. Other noticeable information is the large value of load needed to cause the debonds when $\chi = -0.5$ (C case).

4.2. Position of the first crack onset

Several parametric studies regarding a single fibre configuration subjected to different biaxial loading cases (varying χ) were presented in [3]. In that study, it was shown that for lower values of χ the position, where the debond onset occurs, changes. The onset position was measured by means of the angle θ_0, which is defined as the angle between the radius where the onset is produced and direction of the maximum principal remote stress σ_I^{∞}, see Figure 3(a). For the interface properties used in the present study $\theta_0 = 0°$ for $\chi \gtrsim -0.4$ values, see Figure 4. Thus, it can be concluded that if an isolated fibre is considered θ_0 tends to zero for most of the biaxial cases.

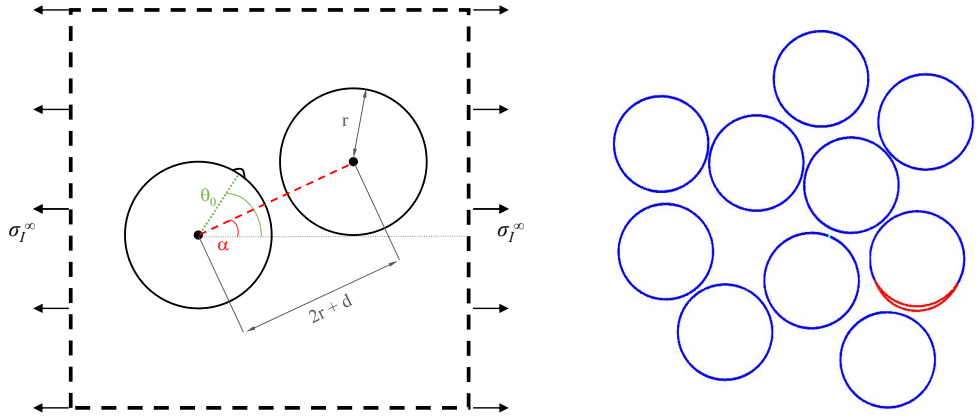

(a) (b)

Figure 3. (a) Definition of angles α and θ_0 in a critical pair of fibres. (b) Deformed shape at the scale of the fibres multiplied by a factor of two, for $\chi = 0.5$(T), corresponding to step number 62 marked with letter A in Figure 2(a).

In the presence of more fibres as is the case of the present study, there are additional parameters that may influence the position where the debond onset occurs [13]. Some of this parameters are the distance between neighbour fibres d, and the angle α given by the line joining two fibre centres and the direction of maximum principal remote stress σ_I^{∞}, see Figure 3(a). The first debond usually occurs at one fibre of a pair of neighbouring fibres with low values of d and α, this pair of fibres is referred as critical pair [13]. In Figure 3(b), the deformed shape at the scale of the fibres multiplied by a factor of two, for $\chi = 0.5$(T), corresponding to step number 62 marked with letter A in Figure 2(a) is presented.

In Figure 4(a), the load biaxility effect on the angles α and θ_0 is depicted. θ_0 values for the single fibre

Excerpt from ISBN 978-3-00-053387-7

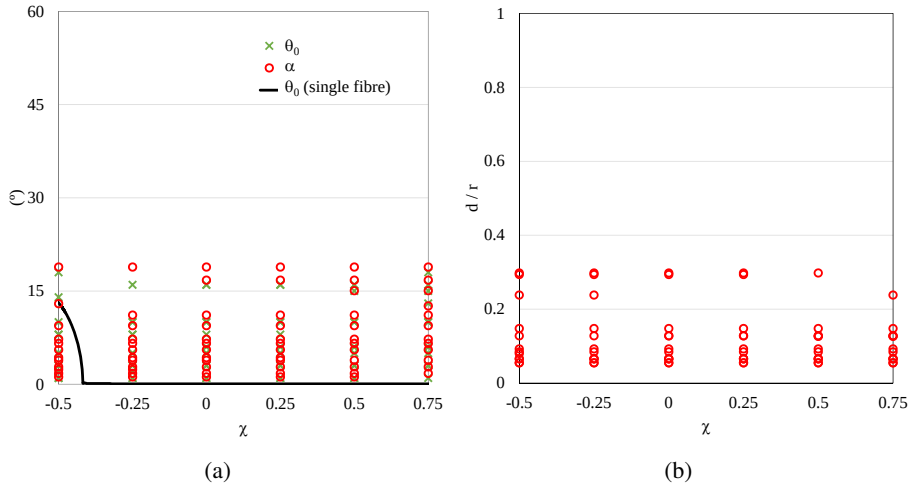

(a) (b)

Figure 4. (a) Load biaxility effect on α and θ_0 for the 10-fibre problem and θ_0 for the single fibre problem [3]. (b) Load biaxility effect on the relative distance between the critical pair of fibres.

problem are also plotted for comparison purposes. Results show that the angle θ_0 is not influenced by the different biaxial loading cases as was for the single fibre case and a scattering occurs for every case. It is interesting to notice that α values seem to be very similar to θ_0 values, both being always lower than 18°. In Figure 4(b), the biaxility effect on the relative distance d/r is presented. Similarly as for the angle θ_0, d is not influenced by the different biaxial loading cases as a quite uniform scatter of its values is observed. Results show that the distances between fibres in a critical pair are always lower than 30% of the fibre radius.

In Figure 5(a), α values are plotted versus θ_0 values. The trend line shows a strong correlation between α and θ_0 values, actually these values are almost identical. Some of the observed differences may be explained by the discretization used to model the fibre-matrix interface (the element size is 2°), while θ_0 must correspond to a boundary element node, α may take any value. Finally, the influence of the distance d in a critical pair on the relative position of the fibres (given by the angle α) is presented in Figure 5(b). Although the scatter of the α values is high, it seems that for lower values of d larger values of α can be obtained, while for larger values of d smaller values of α are needed.

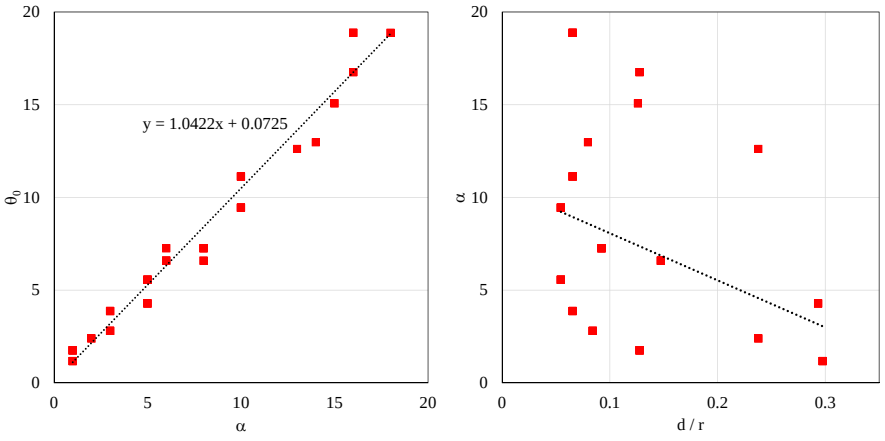

(a) (b)

Figure 5. (a) Correlation between the values of angles α and θ_0. (b) The angle α versus the relative distance between the critical pair of fibres d.

Excerpt from ISBN 978-3-00-053387-7

These results show that the most important parameter for the debond onset position θ_0 in a fibre bundle becomes the configuration of a critical pair (given by the parameters d and α).

The value of θ_0 is very important as the debond growth occurs in a quite symmetrical manner. Thus, the position of the crack onset seems to have a great influence on the final macro–crack path shape.

5. Conclusion

A Linear Elastic-Brittle Interface Model (LEBIM) has been used to characterize the concurrent onset and growth of debonds in a fibre bundle embedded in an infinite matrix subjected to far field biaxial transverse loads. The problem of ten circular inclusions under biaxial transverse loading assuming material properties of a common composite material (glass fibre and epoxy matrix) and the LEBIM has been solved by the collocational BEM, which is very suitable for solving problems with nonlinearities at interfaces.

From the numerical results presented it can be seen that, after reaching a critical load, the interface crack growth at a fibre becomes unstable. A series of peaks and valleys appear in the plot of the applied load versus the total fracture path length, each one corresponding to a fibre debond. The sequence of the obtained debonds clearly tends to form a macro-crack if the coalescence of these interface cracks may occur.

After reaching the critical load, more than one debond is produced in some cases for the same load, while in the other cases a larger load is necessary to produce the following debonds. In the latter cases, the critical load value for the first debond onset gives just an approximation from below of the failure load in the problem under study (the load necessary to produce a macro-crack). The critical loads σ_{cx}^{∞} and σ_{cy}^{∞} (the ones producing the first debond) seem to be related with the relative proximity between fibres taking into account the load direction (the direction of maximum principal remote stress σ_I^{∞}). Thus, the failure load values are lower for the fibre bundle than for the single fibre model. A study of the influence of the load biaxiality ratio χ has also been carried out. The numerical results show that compressions in the x-direction enable crack onset for lower tension loads in the y-direction. The presence of tensions in the x-direction implies that larger loads in the y-direction are required to cause crack onset. The most critical condition seems to appear for $\chi = 0$ (equibiaxial tension-compresion case also known as pure shear).

The present numerical results confirm the conclusions of the previous studies of fibre-matrix debond under biaxial transverse loading in [8–11]. The novelty of the present model based on the LEBIM formulation consists in its capability of quantitative predictions about the concurrent fibre-matrix debond onset and mixed-mode interface crack growth in a fibre bundle.

Acknowledgements

The work was supported by the Junta de Andalucía and European Social Fund (Project of Excellence P12-TEP-1050) and Spanish Ministry of Economy and Competitiveness and European Regional Development Fund (Projects MAT2012-37387, DPI2012-37187 and MAT2015-71036-P).

References

[1] Z. Hashin. Thin interphase/imperfect interface in elasticity with application to coated fiber composites. *Journal of the Mechanics and Physics of Solids*, 50:2509–2537, 2002.

[2] L. Távara, V. Mantič, E. Graciani, and F. París. BEM analysis of crack onset and propagation

Excerpt from ISBN 978-3-00-053387-7

along fiber-matrix interface under transverse tension using a linear elastic-brittle interface model. *Engineering Analysis with Boundary Elements*, 35:207–222, 2011.

[3] V. Mantič, L. Távara, A. Blázquez, E. Graciani, and F. París. Crack onset and growth at fibre-matrix interface under biaxial transverse loads using a linear elastic-brittle interface model. *International Journal of Fracture*, 195:15–38, 2015.

[4] A. Needleman. A continuum model for void nucleation by inclusion debonding. *Journal of Applied Mechanics*, 54:525–532, 1987.

[5] A. Carpinteri, M. Paggi, and G. Zavarise. Snap-back instability in micro-structured composites and its connection with superplasticity. *Strength, Fracture and Complexity*, 3:61–72, 2005.

[6] V. Mantič. Interface crack onset at a circular cylindrical inclusion under a remote transverse tension. Application of a coupled stress and energy criterion. *International Journal of Solids and Structures*, 46:1287–1304, 2009.

[7] M. Braccini and M. Dupeux. *Mechanics of Solid Interfaces*. Wiley, 2012.

[8] F. París, E. Correa, and J. Cañas. Micromechanical view of failure of the matrix in fibrous composite materials. *Composites Science and Technology*, 63:1041–1052, 2003.

[9] V. Mantič and I.G. García. Crack onset and growth at the fibre-matrix interface under remote biaxial transverse loads. Application of a coupled stress and energy criterion. *International Journal of Solids and Structures*, 49:2273–2290, 2012.

[10] E. Correa, F. París, and V. Mantič. Effect of the presence of a secondary transverse load on the inter-fibre failure under tension. *Engineering Fracture Mechanics*, 103:174–189, 2013.

[11] E. Correa, F. París, and V. Mantič. Effect of a secondary transverse load on the inter-fibre failure under compression. *Composites Part B: Engineering*, 65:57–68, 2014.

[12] M. Muñoz-Reja, L. Távara, V. Mantič, and P. Cornetti. Crack onset and propagation at fibre-matrix elastic interfaces under biaxial loading using finite fracture mechanics. *Composites Part A: Applied Science and Manufacturing*, 82:267–278, 2016.

[13] L. Távara, V. Mantič, E. Graciani, and F. París. Modelling interfacial debonds in unidirectional fibre-reinforced composites under biaxial transverse loads. *Composite Structures*, 136:305–312, 2016.

[14] S. Krenk. Energy release rate of symmetric adhesive joints. *Engineering Fracture Mechanics*, 43:549–559, 1992.

[15] S. Lenci. Analysis of a crack at a weak interface. *International Journal of Fracture*, 108:275–290, 2001.

[16] K. Shahin and F. Taheri. The strain energy release rates in adhesively bonded balanced and unbalanced specimens and lap joints. *International Journal of Solids and Structures*, 45:6284–6300, 2008.

[17] A. Carpinteri, P. Cornetti, and N. Pugno. Edge debonding in FRP strengthened beams: Stress versus energy failure criteria. *Engineering Structures*, 31:2436–2447, 2009.

[18] J. W. Hutchinson and Z. Suo. *Mixed mode cracking in layered materials*, volume 29 of *Advances in Applied Mechanics*. Academic Press: New York, 1992.

Excerpt from ISBN 978-3-00-053387-7